Preliminary study of detecting neoplastic growths *in vivo* with real time calibrated autofluorescence imaging

Tao Wu and Jianan Y. Qu

Department of Electrical and Electronic Engineering, Hong Kong University of Science and Technology, Clear Water Bay, N.T., Hong Kong SAR, P. R. China
eequ@ust.hk

Tak-Hong Cheung, Keith Wing-Kit Lo and Mei-Yung Yu

Department of Obstetrics and Gynecology, Chinese University of Hong Kong, Prince of Wales Hospital, Shatin, N.T., Hong Kong SAR, P. R. China

Abstract: The goal of this study was to evaluate the capabilities of a calibrated autofluorescence imaging method for detecting neoplastic lesions. An imaging system that records autofluorescence images calibrated by the cross-polarized reflection images from excitation was instrumented for the evaluation. Cervical tissue was selected as the living tissue model. Sixteen human subjects were examined *in vivo* with the imaging system before routine examination procedures. It was found that calibrated autofluorescence signals from neoplastic lesions were generally lower than signals from normal cervical tissue. Neoplastic lesions can be differentiated from surrounding normal tissue based on the contrast in the calibrated autofluorescence. The effects of the optical properties of tissue on the calibrated fluorescence imaging were investigated.

OCIS codes: (170.6510) Spectroscopy, tissue diagnostics; (170.3890) Medical optics

References and Links

1. R. Richards-Kortum and E. Sevick-Muraca, "Quantitative optical spectroscopy for tissue diagnosis," Ann. Rev. Phy. Chem. **47**, 555-606 (1996).
2. G. A. Wagnieres, W. M. Star and B.C. Wilson, "*In vivo* fluorescence spectroscopy and imaging for oncological applications," Photochem. Photobiol. **68**, 603-32 (1998).
3. N. Ramanujam, "Fluorescence spectroscopy of neoplastic and non-neoplastic tissues," Neoplasia **2**, 89-117 (2000).
4. R.M. Cothren, R.R. Richards-Kortum, M.V. Sivak, M. Fitzmaurice, R.P. Rava, G.A.Boyce, G.B. Hayes, M. Doxtader, R. Blackman, T. Ivanc, M.S. Feld, and R.E. Petras, "Gastrointestinal tissue diagnosis by laser-induced fluorescence spectroscopy at endoscopy," Gastrointest. Endosc. **36**, 105-111 (1990).
5. J, Qu, C. MacAulay, S. Lam and B. Palcic, "Laser-induced fluorescence spectroscopy at endoscopy: tissue optics, Monte Carlo modeling, and in vivo measurements," Opt. Eng. **34**, 3334-3343 (1995).
6. M. Zellweger, P. Grosjean, D. Goujon, P. Monnier, H. van den Bergh and G. J. Wagnieres, "In vivo autofluorescence spectroscopy of human bronchial tissue to optimize the detection and imaging of early cancers," J. Biomed. Opt. **6**, 41-51 (2001).
7. N. Ramanujam, M.F. Mitchell, A. Mahadevan, S. Thomsen, E. Silva and R. Richards-Kortum, "Fluorescence spectroscopy: a diagnostic tool for cervical intraepithelial neoplasia (CIN)," Gynecol. Oncol. **52**, 31-38 (1994).
8. R. Drezek, K. Sokolov, U. Utzinger, I. Boiko, A. Malpica, M. Follen and R. Richards-Kortum, "Understanding the contributions of NADH and collagen to cervical tissue fluorescence spectra: Modeling, measurements, and implications," J. Biomed. Opt. **6**, 385-396 (2001).
9. I. Georgakoudi, B. C. Jacobson, M. G. Muller, E. E. Sheets, K. Badizadegan, D. L. Carr-Locke, C. P. Crum, C. W. Boone, R. R. Dasari, J. Van Dam and M. S. Feld, "NAD(P)H and collagen as in vivo quantitative fluorescent biomarkers of epithelial precancerous changes," Cancer Res. **62**, 682-687 (2002).
10. K. Izuishi, H. Tajiri, T. Fujii, N. Boku, A. Ohtsu, T. Ohnishi, M. Ryu, T. Kinoshita and S. Yoshida, "The histological basis of detection of adenoma and cancer in the colon by autofluorescence endoscopic imaging," Endoscopy **31**, 511-516 (1999).

#2026 - $15.00 US Received January 17, 2003; Revised February 06, 2003

11. M. Kobayashi, K. Shibuya, H. Hoshino and T. Fujisawa, "Spectroscopic analysis of the autofluorescence from human bronchus using an ultraviolet laser diode," J. Biomed. Opt. **7**, 603-608 (2002).
12. J. Y. Qu, Z. J. Huang and J. W. Hua, "Excitation and collection geometry insensitive fluorescence imaging of tissue-simulating turbid media," Appl. Opt. **39**, 3344-3356 (2000).
13. J. Y. Qu, J. W. Hua and Z. J. Huang, "Correction of Geometrical Effects on Fluorescence Imaging of Tissue," Opt. Commun. **176**, 319-326 (2000).
14. J. Y. Qu and J. W. Hua, "Calibrated fluorescence imaging of tissue *in vivo*," Appl. Phys. Lett. **78**, 4040-4042(2001).
15. S. Jutamulia and T. Asakura, "Reduction of coherent noise using various artificial incoherent soures," Optik **70**, 52-57 (1985).
16. A. Agrawal, C. Brookner, M. F. Mitchell and R. Richards-Kortum, "Fluorescence spectroscopy of the cervix: Influence of acetic acid, cervical mucus, and vaginal medications," Laser Surg. Med. **25**, 237-249(1999)
17. Q. G. Zhang, M. G. Muller, J. Wu and M. S. Feld, "Turbidity-free fluorescence spectroscopy of biological tissue," Opt. Lett. **25**, 1451-1453 (2000).
18. M. G. Muller, I. Georgakoudi, Q. G. Zhang, J. Wu and Feld MS, Intrinsic fluorescence spectroscopy in turbid media: disentangling effects of scattering and absorption," Appl. Opt. **40**, 4633-4646 (2001).
19. S. P. Lin, L. H. Wang, S. L. Jacques and F. K. Tittel, "Measurement of tissue optical properties by the use of oblique-incidence optical fiber reflectometry," Appl. Opt. **36**, 136-143 (1997).
20. L. V. Wang and S. L. Jacques, "Source of error in calculation of optical diffuse reflectance from turbid media using diffusion theory," Comput. Meth. Prog. Bio. **61**, 163-170 (2000).

1. Introduction

Conventional diagnosis and screening tools for early detection of neoplastic growth (neoplasia) such as white-light endoscopy have significant limitations because of their poor sensitivity. In this regard, major work continues in the development and evaluation of alternative diagnostic techniques. Optical spectroscopic imaging is being investigated as a non-invasive method for detection of pre-cancerous tissues. Its diagnostic potential is based on the ability to detect changes in both tissue chemistry and tissue architecture. Over past two decades, one of the most extensively investigated applications of optical spectroscopy has been to use fluorescence to detect endoscopically invisible early neoplasia in epithelial tissue sites, which signals pre-malignant changes such as dysplasia and carcinoma *in situ* (CIS). Investigations of fluorescence intensity and spectral characteristics have been performed at many organ sites. Comprehensive reviews of the application of fluorescence spectroscopy in tissue diagnosis are given in Ref. [1-3].

A general observation in the investigation of tissue autofluorescence is that under the same illumination condition, normal tissues almost always more efficiently emit the fluorescence than do neoplastic or cancerous lesions. A study of the human colon indicated that the calibrated fluorescence intensity of normal tissue within an individual is 2 to 3 times higher than that of an adenoma [4]. Calibrated fluorescence intensity from normal bronchial tissue was found to be 2 to 3 times higher than that from bronchial dysplasia and CIS [5,6]. Studies on the cervix demonstrated that the calibrated fluorescence intensity from normal tissue is 2 times higher than that from the abnormal tissue [7]. Results from *in vivo* and *in vitro* investigations on the autofluorescence of cervical tissue demonstrated that the reduction of fluorescence intensity in early cervical lesions is caused by decreases in signal from collagen, the dominant fluorophore in tissue [8,9]. Investigations in the human bronchus and colon revealed that decreased fluorescence in early lesions appears to come from a decrease in collagen and elastin fluorescence due to the screening effect of mucosal thickening or replacement of submucosa by cancer cells [10,11]. The evidences from the *in vivo* and *in vitro* investigations discussed above confirm that the fluorescence intensity carries diagnostic information and may be used in differentiating neoplastic lesions from normal tissues.

Autofluorescence spectroscopy with multiple optical fiber sensors to deliver the excitation light and collect back-scattered fluorescence signals have been successfully used to detect early neoplastic lesions at different organ sites [4-7]. In practice, the distal tip of the fiber sensor gently touches the tissue surface to ensure constant measurement geometry and to produce calibrated fluorescence signals. However, in the examination of large areas of tissue using a conventional imaging system, the recorded fluorescence signals are distorted by

#2026 - $15.00 US Received January 17, 2003; Revised February 06, 2003

geometrical effects (such as varying separation of the source-sample-detector and incident/emission angles over the imaged tissue surface). Without a mechanism to compensate for the geometrical effects, the measured fluorescence intensity can not be directly used for diagnosis purposes.

We recently developed a technique that combines polarization and fluorescence imaging to correct for the geometrical effects and to recover the distribution of intrinsic fluorescence intensity over the imaged tissue surface [12,13]. A cross-polarization arrangement for illumination and collection is used to extract the diffusive components from the reflection of the excitation light. The diffusive reflection reveals information about the excitation and collection geometry. It has been shown that the geometrical effects of fluorescence imaging could be calibrated to a great extent from taking the ratio of the fluorescence signal (F) to diffusive reflection signal (R) of the excitation light recorded from the same site. In an *in vivo* study of calibrated fluorescence imaging from the oral cavity and oropharynx sites, we demonstrated that F/R ratio value is proportional to the intensity of tissue fluorescence and different tissues could be clearly separated using the contrast in F/R value [14]. In this study, we instrumented a colposcope system based on combined fluorescence and cross-polarized reflection imaging to detect squamous intra-epithelial lesions *in vivo*. The potential of the new imaging method for differentiating neoplastic growths from normal tissue was investigated. The ultimate goal of this imaging method is to guide biopsy in real time at various tissue regions.

2. Materials and methods

A schematic of the combined fluorescence and cross-polarized reflection imaging system is shown in Fig. 1. A laser with a 457 nm wavelength (58 BLS series, Melles Griot, CA) was used as the excitation source. The laser light was delivered to the tissue surface through an illumination optical system consisting of a multimode optical fiber of 200μm in diameter, a collimation lens and a linear polarizer. A small part of the fiber (~5 mm in length) was driven by a voice coil at a frequency about 300 Hz to randomize the phases of propagating modes in the fiber and to average out the laser speckle [15]. The illumination spot was about 25 mm in diameter. The excitation power was in the range from 60 mW to 150 mW because the autofluorescence intensity varied from individual to individual. The fluorescence and reflection signals from the sample were collected by a colposcope-like imaging system with a working distance of 400 mm. A dichroic mirror with a cut-on wavelength of 470 nm (470DRLP, Omega Optical, VT) divided the F and R signals collected by the imaging optics into the fluorescence and reflection channels. An additional band-pass filter was used in the fluorescence channel to reject the residual excitation light. The raw fluorescence image was recorded with an ICCD camera (Super Gen II Low light-level Image Sensor, Delft Electronic Products, the Netherlands). A polarizer (P) with its polarization axis perpendicular to the illumination channel was placed in the reflection channel. The cross-polarized reflection image was recorded with a CCD camera (TM-6EG series, Pulnix, CA). The responses from both the fluorescence and reflection channels were calibrated using a tissue phantom. Detailed information on the optical and fluorescence properties of the tissue phantoms were discussed in Ref. [12]. The excitation power was monitored with a dual-channel power meter (Model 2832-C, Newport, CA) during the calibration procedure.

The CCD and ICCD video signals were captured with a fast frame grabber (Genesis-LC, Matrox, Canada). The F/R ratio matrix was created by normalizing the fluorescence image to the cross-polarized reflection image. The 2-D matrix was then multiplied with a scaling constant to be converted into an 8-bit image. A vision processor (Genesis-plus, Matrox, Canada) was used to produce the F/R images at a frame rate of 11 f/s. The system displayed processed images on a separate monitor in two different modes. In first display mode, the fluorescence, cross-polarized reflection and F/R ratio images were simultaneously displayed in three of four quadrants of the monitor. In the second mode, the F/R image was superimposed on the real-time reflection image captured by CCD. A thresholding function

#2026 - $15.00 US Received January 17, 2003; Revised February 06, 2003

allowed only the area with low F/R values to be superimposed on the real-time image. This made a guided biopsy possible.

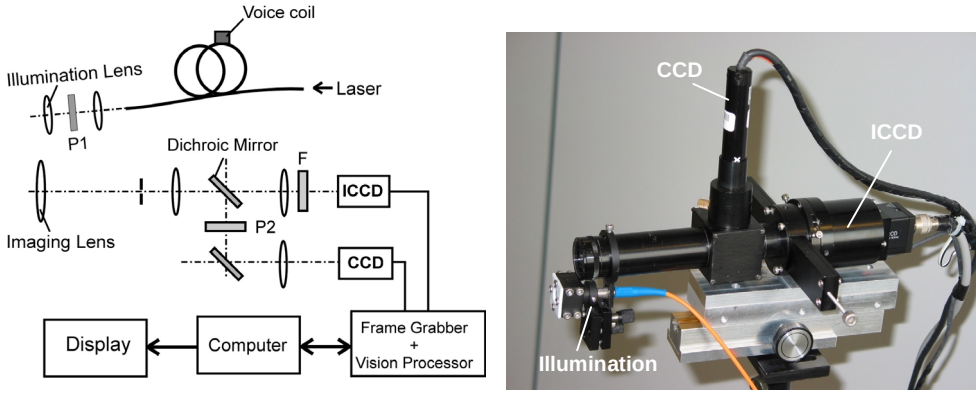

(a) (b)

Fig. 1. (a) A schematic of the F/R colposcopic imaging system. P1 and P2 are the polarizers with their polarization orientations perpendicular to each other. F is the filter to remove the residual reflection of the excitation light. (b) Picture of actual imaging head.

Sixteen human subjects originally scheduled for the loop electrosurgical excision procedure (LEEP) were enrolled in the *in vivo* investigation of the F/R imaging technique. The cervix is normally covered with a layer of mucus that may alter the spectral characteristics of both the fluorescence and reflectance [16]. To avoid interference from the cervical mucus, the surface of the cervix was first cleaned with PBS before examination with the F/R imaging system. The fluorescence, reflection and F/R images from different angles were recorded and stored for post-analysis. A routine colposcopy was made after the fluorescence examination. Histological analysis of the tissue samples taken from the four quadrants of the subjects' cervices was performed by experienced pathologists. This study was approved by the Ethical Committee of the Prince of Wales Hospital, the Chinese University of Hong Kong. Consent letters were obtained from all the patients enrolled in this study.

3. Results and discussion

Figure 2 displays typical results obtained from the fluorescence examination with the imaging system shown in Fig. 1. Here, a band-pass filter with its central wavelength and bandwidth at 480±15 nm, close to the excitation wavelength, was used in the fluorescence channel to collect fluorescence images. This ensured that the optical properties of the tissue at the fluorescence band were close to those at the excitation. We observed that the F/R value remained constant when the illumination conditions, including the imaging angle and excitation power, were varied. The areas of tissue with lower F/R value were well defined in the F/R images which were presented in pseudo color. On the contrary, the areas of tissue with low fluorescence intensity could not be clearly identified in the corresponding raw fluorescence images because of geometrical effects. The histological examination of the tissue samples indicated that the tissue area with a lower F/R value in the upper part of cervix shown in Fig. 2 appeared to be low-grade squamous intra-epithelial lesion (SIL). The tissue area with the lower F/R value in the lower part of cervix shown in the same figure was found to be high-grade SIL or cervical intraepithelial neoplasia II-III (CIN II-III).

#2026 - $15.00 US Received January 17, 2003; Revised February 06, 2003

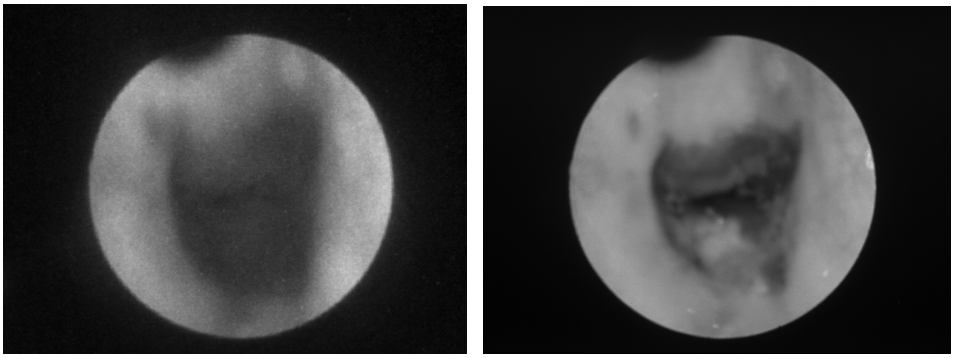

(a) (b)

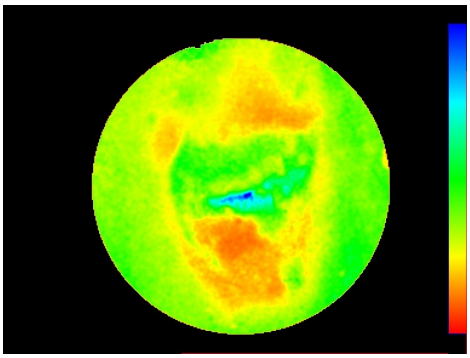

(c)

Fig. 2. Typical results obtained from a subject with low-grade SILs and high-grade SILs. (a) raw fluorescence image; (b) cross-polarized reflection image; (c) F/R ratio image.

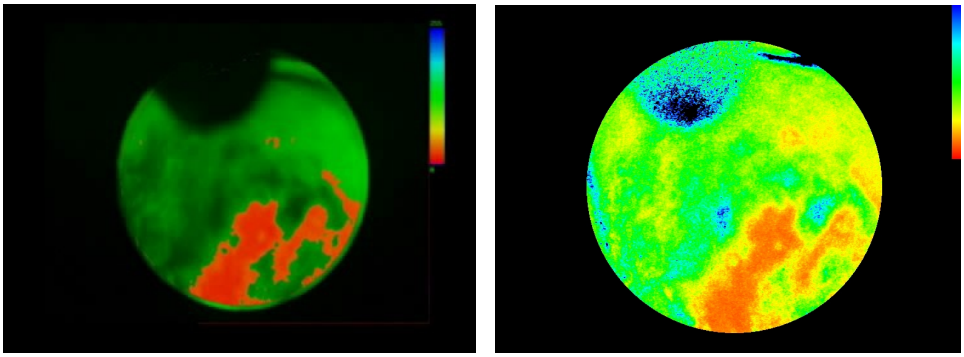

(a) (b)

Fig. 3. F/R ratio image superimposed with real-time reflection image for guided biopsy. (a) (1.6 MB) Video clip of guided biopsy; (b) F/R ratio image.

Figure 3 shows the F/R imaging using the display mode with the F/R ratio image superimposed on the real-time reflection image captured by CCD. This function was designed to make guided biopsy possible. In the superimposition display mode, tissue areas with F/R values higher than a pre-set threshold become transparent. When the threshold is set properly, only tissue areas with low F/R values are superimposed on the real-time reflection image for guiding the biopsy. The video clip in Fig. 3(a) demonstrates the guided biopsy

#2026 - $15.00 US Received January 17, 2003; Revised February 06, 2003

procedure using the F/R colposcopic imaging system. The real-time reflection image was displayed in green color. As shown in the video clip, the tissue specimen was accurately taken from the area of interest (with a low F/R ratio value). The dark area in the upper part of the image was caused by the shadow of speculum. As a reference, an F/R image taken from the same tissue site as in the video clip is displayed in Fig. 3(b).

The biopsy specimens collected from the 16 subjects enrolled in this study exhibited normal, human papilloma virus (HPV) infection and neoplastic growths, respectively. An image processing program was used to calculate the mean and standard deviation of the F/R value over the area of tissue taken for histological analysis. Figure 4 shows the average F/R values of the normal and abnormal tissues (HPV infection, CIN I and CIN II-III) from all 16 patients. For the patients with lower F/R values around squamous-columnar junctions in all four quadrants, the F/R value in the tissue area away from the junctiosn and exhibiting colposcopically normal was calculated to represent the F/R signal of normal tissue. Here, the absolute value of the F/R ratio was dependent on the scaling factor for display. Thus, the average F/R value varies from patient to patient. However, in most cases the F/R value for abnormal tissue is lower than that for normal tissue for an individual subject except case 3, 5 and 12. The contrast of F/R values for an individual subject can then be used to detect abnormal tissue.

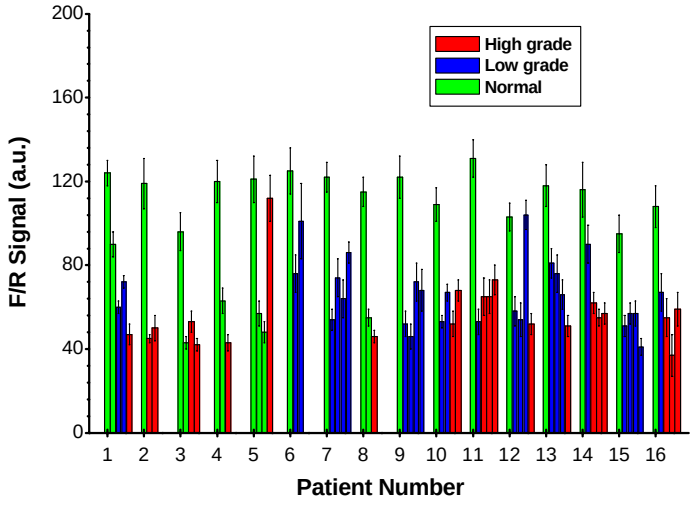

Fig. 4. Bar chart illustration of the mean values of the F/R ratio for the examined cervical tissues from 16 subjects.

To determine how accurately the F/R imaging method differentiated abnormal tissue from normal tissue, we set the threshold to a variety of F/R value percentages measured from normal tissue for each individual subject. A sensitivity of 89% and specificity of 77% to separate abnormal tissue from normal tissue was achieved when the threshold was set to 70% of the F/R value measured from normal tissue. However, the difference in F/R values between low-grade SILs (HPV infection and CIN I) and high-grade SILs (CIN II-III) is not significant as shown in Fig. 4. The separation of high-grade SILs from low-grade SILs is poor.

It is well known that the interplay of tissue's absorption and scattering properties affects the measured tissue's autofluorescence and reflectance signals. To understand the effects of the optical properties of tissue on F/R imaging, we begin with a method recently reported by a research group from MIT [17,18]. This method was based on photon migration theory and was developed to recover intrinsic fluorescence using simultaneously measured fluorescence

#2026 - $15.00 US Received January 17, 2003; Revised February 06, 2003

and reflectance signals. Here, we use the theory to relate the intrinsic fluorescence to the F/R ratio as follow:

$$f(\lambda_{em}) = \frac{\mu_s^{ex} l \cdot R^0(\lambda_{ex})}{\left(\frac{R^0(\lambda_{ex})R^0(\lambda_{em})}{\varepsilon(\lambda_{ex})\varepsilon(\lambda_{em})}\right)^{1/2}\left(\frac{R(\lambda_{em})}{R^0(\lambda_{em})}+\varepsilon(\lambda_{em})\right)} \cdot \frac{F(\lambda_{em})}{R(\lambda_{ex})} \quad (1)$$

where $F(\lambda_{em})$ is the fluorescence signal from a tissue at emission wavelength λ_{em}. R and R^0 are the diffused reflectance signals with and without absorption from the tissue, respectively. $F(\lambda_{em})$ and R must be recorded under the same illumination/collection geometry. μ_s^{ex} is the scattering coefficient of the tissue at excitation wavelength λ_{ex}. The parameter ε is related to the illumination/collection geometry and the anisotropy factor of the scattering. The quantity l is another constant related to the illumination/collection scheme. Eq. (1) has been successfully applied to restore intrinsic fluorescence from fluorescence and reflectance measured with an optical fiber sensor.

It has been known that the near-diffusive backscattering contributes to major errors in the theories with the assumption that reflectance is totally diffusive [19,20]. In an F/R imaging system, the cross-polarization arrangement for illumination and collection can effectively reduce the near-diffusive backscattering (photons scattered once or twice) and enhance the diffusive components in total reflectance. To form the F/R image, the fluorescence image and cross-polarized reflection image are collected from the same tissue site. The corresponding pixels in the fluorescence and reflection images then record signals in identical geometries. Therefore, for each individual pixel, the F/R ratio can be related to intrinsic fluorescence using Eq. (1).

In previous experimental studies and Monte Carlo simulations, we have demonstrated that the geometrical effects on fluorescence measurements can be corrected well by using F/R ratio [12-14]. In optically homogeneous tissue, the intrinsic fluorescence image was linearly proportional to F/R ratio image regardless of the variation in the illumination/collection geometry over the tissue surface. This indicates that the geometrical parameters in Eq. (1) are not sensitive to the F/R imaging system. The parameters can then be treated as constants for all the pixels in the fluorescence and reflection images. The first term on the right side of Eq. (1) is then dependent only on the optical properties of tissue and can be used to discuss the effects of optical properties on F/R imaging.

In the F/R imaging system shown in Fig. 1, the fluorescence image was collected in a wavelength band close to the excitation wavelength. With the approximation of $\lambda_{ex} \approx \lambda_{em}$, Eq. (1) can be simplified as:

$$f \approx \frac{\mu_s \varepsilon l}{\left(\frac{R}{R^0}+\varepsilon\right)} \cdot \frac{F}{R} \quad (2)$$

where R and R^0 are the reflectance at the excitation wavelength with and without absorption, respectively. The ratio of R/R^0 is determined only by the optical properties of the tissue and independent of the imaging geometry because both R and R^0 are assumed to be diffusive. The first term on the right side of Eq. (2) determines the effects of the optical properties of the tissue on F/R imaging. When the absorption coefficient is constant, the F/R value is inversely proportional to the scattering coefficient. This is consistent with a previous experimental study on tissue phantoms [14]. With a fixed scattering coefficient, the F/R value decreases monotonically with increases in absorption. This result agrees with the experimental observations only when the absorption is small and scattering dominates the light transport in the tissue phantoms [14].

#2026 - $15.00 US Received January 17, 2003; Revised February 06, 2003

In other extreme conditions, the fluorescence is considered to be collected in a long wavelength band (e.g., $\lambda > 600$ nm) where blood absorption is low and negligible. This makes R/R^0 nearly a constant ~ 1. Equation (1) then becomes:

$$f(\lambda_{em}) \approx \frac{\mu_s^{ex} l(\varepsilon(\lambda_{ex})\varepsilon(\lambda_{em}))^{1/2} R^0(\lambda_{ex})}{\left(R^0(\lambda_{ex})R^0(\lambda_{em})\right)^{1/2}(1+\varepsilon(\lambda_{em}))} \cdot \frac{F(\lambda_{em})}{R(\lambda_{ex})} \tag{3}$$

Note that the first term on the right side of the Eq. (3) is only determined by the scattering property of tissue. It is independent on the blood absorption and imaging geometry. This means that the inhomogeneity of blood in tissue does not affect the relationship between intrinsic fluorescence and the F/R ratio. This is the major advantage of using a long wavelength fluorescence image. The possible disadvantages are that the collagen signal in long wavelength region is weak and not dominant. Signals from other fluorophores, such as flavin and porphyrin, may create significant interference. Also, the transport distance of photons in the long wavelength region (> 600 nm) is significantly longer than the excitation wavelength (457 nm). The F/R ratio may produce artifacts in tissues with surface curvatures or blood distribution varying rapidly over the imaged tissue area.

4. Conclusion

We investigated the potential of the F/R imaging technique for detecting neoplastic lesions *in vivo*. Human cervical tissue was used as the living tissue model for the study. The results demonstrate that the F/R ratio corrects the geometrical effects on fluorescence measurements and enhances the contrast between abnormal and normal tissue. The F/R value can be used to detect abnormal tissue. However, the differentiation of high-grade lesions from low-grade lesions is poor. The effects of the optical properties of tissue on F/R imaging were discussed. It was found that variation in both scattering and absorption properties of tissue over imaged tissue surfaces introduce artifacts in F/R imaging to a certain degree. A method to minimize the possible interference from the inhomogeneity of blood distribution was proposed. In future studies, our efforts will be focused on the development of a method to minimize the effects of optical properties of tissue on the combined autofluorescence and cross-polarized reflection imaging. Also, an endoscope system with a cross-polarization arrangement will be developed to investigate the potential of F/R imaging to detect neoplastic growths at other organ sites.

Acknowledgements

The authors acknowledge support from the Hong Kong Research Grants Council through grants HKUST6052/00M and HKUST6025/02M.

#2026 - $15.00 US Received January 17, 2003; Revised February 06, 2003